γ OG 1014

CONF-8708166--7

HELIOS note 286
1.3.1988
BNL-41265

Spectra of Negative Particles and Photons in Collisions of p–W and ^{16}O –W at 200 GeV/u

DE88 011254

H.-W. Bartels
Phys. Inst. d. Univ. Heidelberg
W.-Germany
HELIOS COLLABORATION

Abstract

$p_\perp$ spectra of negative particles were measured for p–W and ^{16}O –W collisions at 200 GeV/u in the rapidity range $0.9 < y < 1.9$. Within the systematic errors of 20% the spectra are identical in the range $0.05 < p_\perp < 2.0$ GeV/c. The p–W and ^{16}O –W spectra exhibit an exponential shape for $p_\perp > 250$ MeV/c. This is consistent with previous p–A data, but there is a significant excess above this exponential at lower $p_\perp$.

Photon spectra were measured using a conversion method. Their $p_\perp$ distribution agrees in shape with the sum of known hadronic γ-sources.

1. Introduction

There is currently intense interest in the physical properties of a state of high energy density in nuclear matter. The excitement is driven by the expectation that confinement of the partons in a hadron cannot survive when the density of partons is large compared to the density inside ordinary hadrons. This prospect is supported by QCD calculations [1], and collisions between heavy nuclei at ultrarelativistic energies are predicted to provide the energy densities required for deconfinement (greater than 2-3 GeV/fm^3). Among the goals of the first experiments with heavy ion beams are investigations of the energy density and spatial extent of the highly excited nuclear fireball to address whether the necessary conditions have been satisfied, and a closer examination of events with large amounts of energy deposited in the target. The HELIOS (High Energy Lepton and Ion Spectrometer) experiment therefore combines 4π calorimetric coverage with measurement of charged particle multiplicity, inclusive particle spectra, two particle correlations, lepton pairs and photons. Data were taken at the CERN SPS, using 200 GeV/u ^{16}O beams and 200 GeV proton beams.

Here we discuss the single particle spectra measured by the HELIOS experiment with a magnetic spectrometer examining the event through a narrow azimuthal gap ($15° < \theta < 45°$) in the calorimeter coverage (External Spectrometer). The momentum distributions of charged particles should be affected by the expansion and subsequent decay of a deconfined state of matter inside the colliding nuclei. The momentum spectra may also indicate the degree of thermalization reached in the collision, and allow a search for evidence of radial flow in the boost of heavy particle spectra, though these boost effects may be quite small if only a partial phase transition to a mixed phase is attained [2]. Photons provide a unique tool to study hadronic interactions as they couple directly to the electric charge of the quarks and escape the collision unaffected by final state interactions or fragmentation processes. Direct photons can be emitted both as thermal radiation from the deconfined state [3], and as coherent bremsstrahlung signaling the slowing-down of the nuclear proton distribution [4].

In this contribution we present the transverse momentum spectra of negatively charged particles, dominantly pions, and photons as measured in the External Spectrometer. Data from oxygen and proton beams with tungsten targets are compared.

2. The Experimental Setup

The external spectrometer (shown in Fig. 1) views the target through a narrow slit in the calorimeter wall, covering the pseudorapidity interval $0.9 < \eta < 2.0$. A magnet with a momentum kick of ~80 MeV/c and two high resolution drift chambers provide the momentum measurement of charged particles. A 5% radiation length converter placed directly in front of the first drift chamber makes it possible to measure photons in the same apparatus via the observation of the converted electron-positron pair. Two planes of multiwire proportional chambers (COMET) bracketing the converter allow localization of the conversion point. A local anticoincidence requiring no signal before the converter and a hit after the converter was used as a photon trigger.

The resolution of the drift chambers measuring the horizontal coordinate via the drift time ($\sigma \simeq 180\ \mu$m) and the vertical coordinate via charge division ($\sigma \simeq 1.0$ cm) allows separation of the background from the calorimeters around the slit. Off-line, a photon is identified by the COMET trigger pattern and a pair of electrons split by the magnetic field. The photons and charged particles must be tracked back through the slit to the target, in order to remove the slit background. The time-of-flight and aerogel Cerenkov counters shown in Fig. 1 provide particle identification but are not used in the data shown here.

3. The Data Sets

Two data samples are presented in this work: p–W and ^{16}O –W interactions, both at 200 GeV/u. For p–W, an active target was used; the potential wires of a drift chamber served as the targets. Off-line analysis determined the wire at which the interaction took place and rejected multiple interactions and interactions outside the target. For ^{16}O –W, a 0.1 mm W disk was used as a passive target. The trigger for these data required a valid interaction, as described in ref.5, and also used the transverse energy measured in the calorimeters in the pseudorapidity range $-0.1 < \eta < 2.9$. Varying scale down factors for the different E_T thresholds were used, providing good statistics across the E_T range. For charged particle data presented from the oxygen sample, only events triggered on $E_T > 110$ GeV ($\simeq 0.6 \cdot 10^5$ interactions) are used, in order to select central collisions. For comparison, a minimum bias sample from p–W collisions was approximated, by using the lowest E_T threshold available, $E_T > 10$ GeV (yielding $\simeq 1.5 \cdot 10^5$ interactions).

The photon data from ^{16}O –W are drawn from the E_T triggered events, resulting in uniform statistical coverage over the entire E_T range. The p–W data were taken with the special photon trigger described above, with a bias against peripheral collisions by requiring $E_T > 20$ GeV.

4. Corrections to the data

The measured $p_\perp$ spectra were corrected for various detector effects, namely decays in flight, geometrical acceptance and the finite momentum resolution ($\Delta p/p^2 = 0.08/GeV$). Pion $p_\perp$ spectra were simulated including all detector properties with the generator described below, and reconstructed using the full analysis chain. The ratio of generator input to simulated spectra is used to correct the data presented below.

The corrections for low $p_\perp$ are dominated by the spectrometer acceptance and are not dependent on the spectral shape. The External Spectrometer has a fixed acceptance in pseudorapidity, yielding a rapidity acceptance that depends on $p_\perp$. We have previously presented data in a fixed range in pseudorapidity [6]. In order to study spectra for a fixed rapidity range with such a device, one must either consider a narrow rapidity band, or correct for acceptance losses for low $p_\perp$ particles. We have investigated both approaches and find that the low $p_\perp$ part of the corrected spectrum for $0.9 < y < 1.9$ looks the same as in the band $0.9 < y < 1.5$ where no kinematical acceptance correction is required. We have therefore used the first band to optimize the statistics in the high end of the $p_\perp$ spectrum, under the assumption that there are no rapid changes in the low $p_\perp$ distribution from $y = 1.5$ to $y = 1.9$. The low $p_\perp$ region is also affected by the decay corrections, which are made under the assumption that the detected negative particles are pions. Other instrumental effects in the reconstruction of low $p_\perp$ tracks, such as multiple scattering and energy loss have been simulated in the Monte Carlo program, and result in small corrections to the spectrum. At large $p_\perp$, the effects of momentum smearing become large, and the correction factors depend on the spectral shape.

To generate Monte Carlo events we used a parametrization combining FNAL and CERN ISR measurements [7] of charged particle spectra taking into account the dependence on the center of mass energy and the rapidity. For the well-known hardening of the $p_\perp$ spectra in p–A collisions, this parametrization was modified using the prescription of Cronin et al. [8]:

$$\frac{d\sigma_{pA}}{dp_\perp} = A^{n(p_\perp)} \cdot \frac{d\sigma_{pp}}{dp_\perp} \tag{4.2}$$

where $n(p_\perp)$ is a function approximately linear for $p_\perp < 3$ GeV. The function $n(p_\perp)$ was measured for $p_\perp > 800$ MeV/c in p–W collisions at 200 GeV [8] . For lower $p_\perp$ no data were available and so the function $n(p_\perp)$ was extrapolated linearly. The rapidity distribution for the generator was assumed to be equal to the one corresponding to the $dE_T/d\eta$ measured by HELIOS [9]. The $p_\perp$ spectra from this generator, including full simulation of the detector response, are consistent with the uncorrected data above $p_\perp \simeq 250$ MeV/c. Therefore we can use the ratio of the generator input to the reconstructed spectrum to correct the data.

The inclusive γ spectra were calculated for the contributions of known hadronic sources. The relevant hadrons and their contributions (normalised to π^0) taken from ISR pp data are: π^0 (100%), η (14.5%), η' (6.3%), ω (11%) [10]. The $p_\perp$ distribution of the π^0 was derived from π^- and π^+ data [7,8]. For the other mesons the $p_\perp$ spectra were derived from the π^0 spectrum assuming scaling of the spectra with the transverse mass [11] $m_\perp = \sqrt{m^2 + p_\perp^2}$ as

$$f(p_\perp;h) = f(p_\perp;\pi^0) \cdot \left(\frac{m_\perp(p_\perp;\pi^0) + 2.0}{m_\perp(p_\perp;h) + 2.0} \right)^{12.3} \quad ; \quad h = \eta, \eta', \omega \qquad (4.3)$$

As above, the rapidity distribution of the hadrons was taken from the calorimeter $dE_T/d\eta$ data [9].

The systematic errors were evaluated by comparing the corrected $p_\perp$ spectra for different regions in pseudorapidity. These spectra agreed within ~15% providing a limit on systematic errors from different positions in the detectors. Small variations of the detector response between the p–W and ^{16}O –W running (efficiencies, resolution) resulted in a deviation of 5% at $p_\perp = 1.5$ GeV/c going up to 15% at the highest $p_\perp$'s (2 GeV/c). Thus the systematic error is estimated to be approximately 20% , but it should be noted that this yields an error in the slope of less than 3% .

5. Results

Figures 2a and b show the $p_\perp$ spectra for negative particles observed in p–W and ^{16}O –W collisions at 200 GeV/u, respectively. These data are in the rapidity range $0.9 < y < 1.9$ and the $p_\perp$ range $0.05 < p_\perp < 2.0$ GeV/c. No absolute cross sections are quoted. The dashed line gives the π^- spectrum from the generator described above, which represents the spectrum expected from p-p collisions modified by nuclear effects [8]. The equivalence at high $p_\perp$ of the p–W data with the generator indicates the expected agreement of our measurement with the previous one [8]. The ratio of the ^{16}O and proton $p_\perp$ spectra is plotted in Fig. 2c as a function of $p_\perp$; the normalization is done according to the integrals under the curves. In the range shown, which covers five orders of magnitude in cross section, the spectra are identical within statistical and systematic errors. Figures 2b and 2c indicate that there are no significant differences in the pion $p_\perp$ spectra for nucleus–nucleus and p–nucleus collisions.

For both ^{16}O and proton data, a deviation from the generator is observed for $p_\perp \lesssim 0.25$ GeV/c. It is important to note that the generator is derived from p-p data, and is corrected for p–A data measured only in the high $p_\perp$ region of the spectrum. Other instrumental effects in the reconstruction of low $p_\perp$ tracks have been simulated in the Monte Carlo program, and result in small corrections to the spectrum.

The observed $p_\perp$ spectra can clearly not be described by a single exponential, however we have looked at the slopes in two narrow regions of $p_\perp$. Assuming an exponential shape one finds an inverse slope of $\approx$ 190 MeV/c in the range of $0.5 < p_\perp < 1.0$ GeV/c and of $\approx$ 85 MeV/c in the range of $0.1 < p_\perp < 0.2$ GeV/c. The rise in cross section at low $p_\perp$ was previously reported in the streamer chamber experiment at CERN [12].

The corrected inclusive γ-spectra are shown in Fig. 3a,b in the range $0.1 < p_\perp < 1.3$ GeV/c and $0.9 < y < 1.9$. The ratio of the ^{16}O to the proton data (Fig. 3c) is constant with $p_\perp$ within the statistical errors. The sum of hadronic sources agrees in shape with the observed $p_\perp$ distribution. A normalisation of the gamma cross section to the charged pions is not yet done. This would be another test for additional photon sources, e.g. thermal radiation originating from interactions between the quarks and gluons in a thermalized state. Under the assumption of a formation of such a thermalized state in high $E_\perp$ events the rate of thermal photons has been estimated to be $\sim$ 10 % of the hadronic background [13].

6. Conclusion

The $p_\perp$ spectra for negative particles and photons were measured for p–W and ^{16}O –W at 200 GeV/u. Within the statistical and systematic errors of $\sim$ 20% the spectra are identical in shape over 5 orders of magnitude, and are well described by the systematic studies of Cronin et al. for p–A at high $p_\perp$. An excess compared to p–p collisions in the $p_\perp$ spectra for $p_\perp < 250$ MeV/c is seen both in p–W and ^{16}O –W collisions.

The shape of the photon spectra obtained so far can be explained by the known hadronic sources. The expected spectral shape for 'thermal' photons, however, is not very different from the hadronic background [13]. Only a careful study of the absolute cross-sections may lead to experimental evidence of such a signal.

We are grateful to the CERN Accelerator Division for the magnificent performance of the machine complex, and would like to thank the staff of the GSI computer center for the resources and invaluable help in the analysis of these data. We thank CERN and our national funding agencies for their support.

This work supported in part by the U.S. Dept. of Energy under contract DE-AC02-76CH00016.

References

1. See, for example, Proc. of the Quark Matter Conferences in Brookhaven (1984), Helsinki (1984) and Asilomar (1986)

   M. Gyulassy, Nucl. Phys. **A418** (1984) 59c.

2. K. Redlich, H. Satz, Phys. Rev. **D33** (1986) 3747.

3. E. L. Feinberg, Nuovo Cimento **A34** (1976) 391.

   L. D. McLerran, T. Toimela, Phys. Rev. **D31** (1985) 545.

   K. Kajantie, H. I. Miettinen, Z. Phys. **C9** (1981) 341.

   E. V. Shuryak, Sov. J. Nucl. Phys. **28(3)** (1978) 408.

4. J. D. Bjorken, L. McLerran, Phys. Rev. **D31** (1985) 63.

5. J. Schukraft, contribution to this conference.

6. U. Goerlach, HELIOS Collaboration, Proceedings of the International Europhysics Conference on High Energy Physics, Uppsala, Sweden, 1987.

7. B. Alper et al., Nucl. Phys. **B100** (1975) 237.

8. D. Antreasyan, J. W. Cronin, H. J. Frisch, M. J. Shocket, Phys. Rev. **D19** (1979) 764.

9. F. Corriveau, contribution to this conference, and

   T. Akesson, et al., to be published in Z. Phys. C.

10. A. Chilingarov et al., Nucl. Phys. **B151** (1979) 29.

    R. Singer et al., Phys. Lett. **B60** (1976) 385.

    C. Kourloumelis et al., Phys. Lett. **B84** (1979) 277.

    M.G. Albrow et al., Nucl. Phys. **B155** (1979) 39.

    M. Diakonou et al., Phys. Lett. **B89** (1980) 432.

    P. Perez et al., Phys. Lett. **B112** (1982) 260.

    M. Basile et al., Nuovo Cimento **A65** (1981) 421.

    T. Akesson, Zeit. f. Phys. **C18** (1983) 5.

11. M. Bourquin and J. M. Gaillard, Nucl. Phys. **B114** (1976) 334.

12. T.J. Humanic, NA35 Collaboration, Proceedings of the International Europhysics Conference on High Energy Physics, Uppsala, Sweden, 1987.

13. M. Neubert, diploma thesis, Heidelberg University, 1988. (unpublished)

Figure captions

Fig. 1 Top view of the external spectrometer in HELIOS

Fig. 2 a) $p_\perp$ spectra of negative particles for p–W at 200 GeV

$E_T > 10$ GeV in $-0.1 < \eta < 2.9$

b) $p_\perp$ spectra of negative particles for ^{16}O –W at 200 GeV/u

$E_T > 110$ GeV in $-0.1 < \eta < 2.9$

c) Ratio of fig. 2a and 2b

The systematic errors are estimated to be about 20%

Only statistical errors bars are shown in the figure

Fig. 3 a) $p_\perp$ spectra of photons for p–W at 200 GeV

$E_T > 20$ GeV in $-0.1 < \eta < 2.9$

b) $p_\perp$ spectra of photons for ^{16}O –W at 200 GeV/u

all E_T-Trigger

c) Ratio of fig. 3a and 3b

The systematic errors are estimated to be about 20%

Only statistical errors bars are shown in the figure

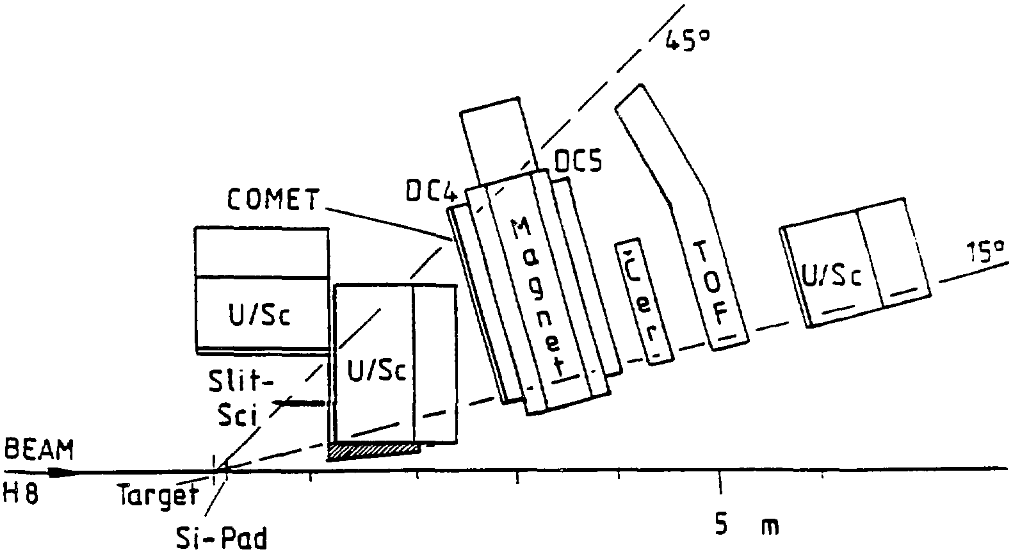
45°
DC5
COMET
DC4
Magnet
Čer.
TOF
U/Sc
U/Sc
U/Sc
15°
Slit-
Sci
BEAM
H8
Target
Si-Pad
5 m

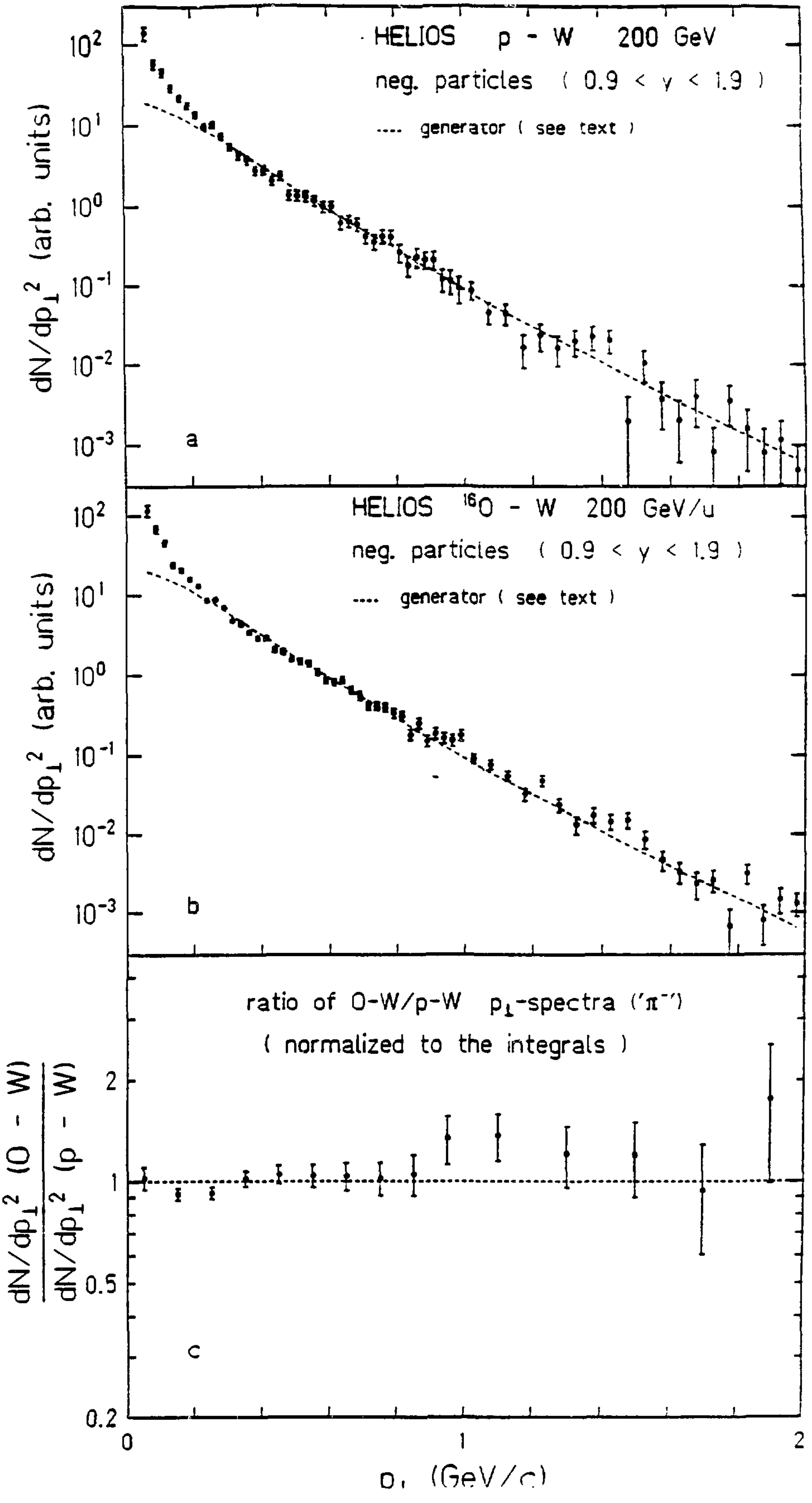
HELIOS p - W 200 GeV
neg. particles (0.9 < y < 1.9)
---- generator (see text)
dN/dp⊥² (arb. units)
10²
10¹
10⁰
10⁻¹
10⁻²
10⁻³
a
HELIOS ¹⁶O - W 200 GeV/u
neg. particles (0.9 < y < 1.9)
---- generator (see text)
dN/dp⊥² (arb. units)
10²
10¹
10⁰
10⁻¹
10⁻²
10⁻³
b
ratio of O-W/p-W p⊥-spectra ('π⁻')
(normalized to the integrals)
dN/dp⊥² (O - W) / dN/dp⊥² (p - W)
2
1
0.5
0.2
c
0
1
2
p⊥ (GeV/c)

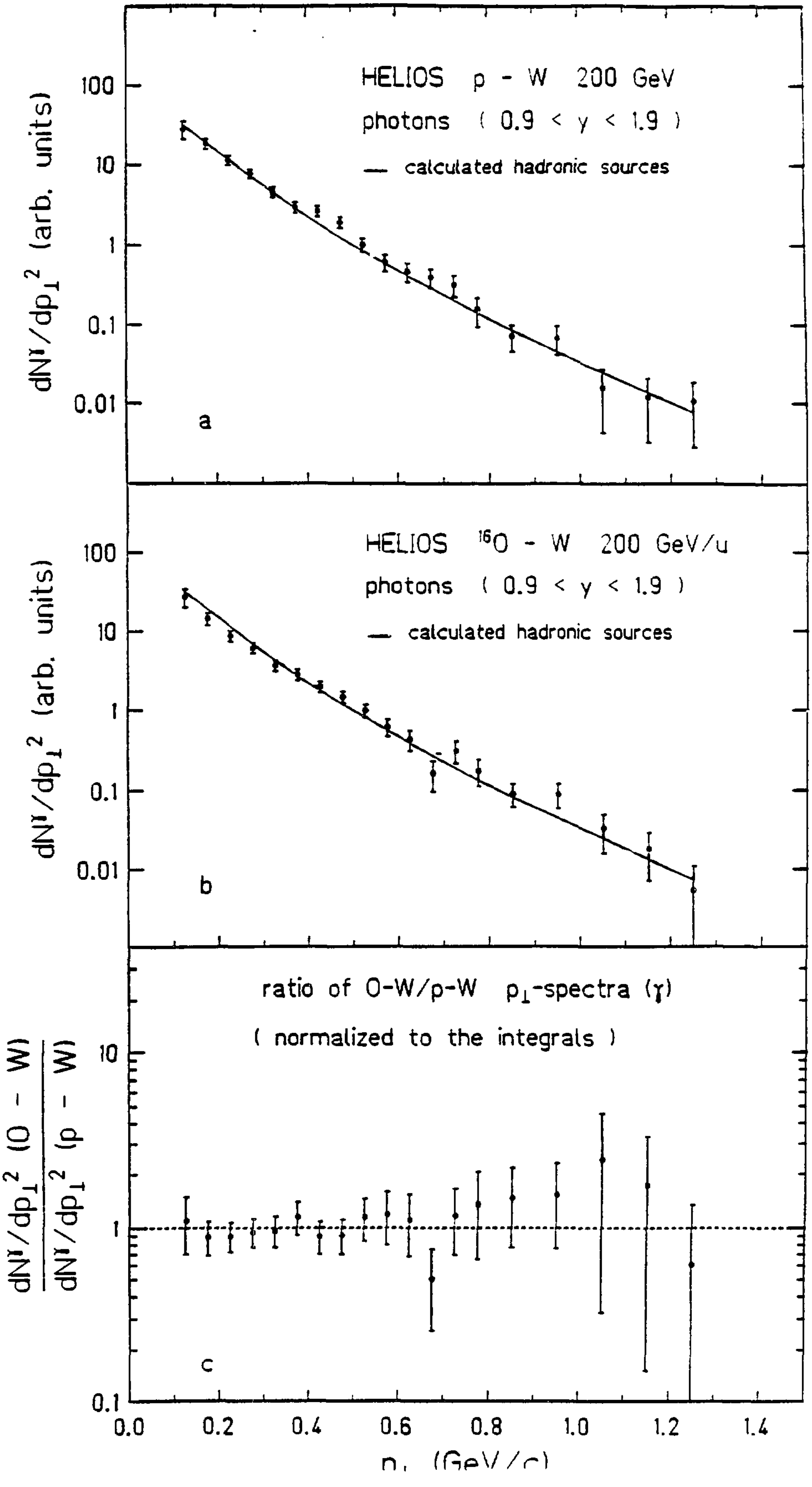
HELIOS p - W 200 GeV
photons (0.9 < y < 1.9)
— calculated hadronic sources
$dN^\gamma/dp_\perp^2$ (arb. units)
100
10
1
0.1
0.01
a
HELIOS ^{16}O - W 200 GeV/u
photons (0.9 < y < 1.9)
— calculated hadronic sources
$dN^\gamma/dp_\perp^2$ (arb. units)
100
10
1
0.1
0.01
b
ratio of O-W/p-W $p_\perp$-spectra (γ)
(normalized to the integrals)
$\frac{dN^\gamma/dp_\perp^2\ (O - W)}{dN^\gamma/dp_\perp^2\ (p - W)}$
10
1
0.1
c
0.0
0.2
0.4
0.6
0.8
1.0
1.2
1.4
$p_\perp$ (GeV/c)